Multiple-Bit Differential Detection of Offset Quadriphase Modulations

M. K. Simon[1]

Analogous to multiple-symbol differential detection of quadrature phase-shift keying (QPSK), a multiple-bit differential detection scheme is described for offset QPSK that also exhibits continuous improvement in performance with an increasing observation interval. Being derived from maximum-likelihood (ML) considerations, the proposed scheme is purported to be the most power-efficient scheme for such a modulation and detection method. Extension of the results to shaped offset QPSK also is considered.

I. Introduction

More than a decade ago, multiple-symbol differential detection of M-ary phase-shift keying (M-PSK) [1] was introduced by the author as a means of improving system performance relative to the traditional (two-symbol observation) differential detection scheme. The technique made use of maximum-likelihood sequence estimation (MLSE) of the transmitted phases rather than symbol-by-symbol detection, and, depending on the number of symbols observed, its performance was shown to span between that of conventional differential detection and ideal coherent detection of differentially encoded M-PSK. Since then, many advancements and applications based on the original contribution in [1] have been reported in the literature, examples of which can be found in [2–10].

One special case of high interest corresponds to $M = 4$, i.e., quadrature phase-shift keying (QPSK), and numerical results were reported in [1] for this case to allow comparison with conventional differential detection of QPSK (DQPSK). By comparison, the literature is quite sparse [11,12] regarding differential detection of offset QPSK (OQPSK) despite the fact that OQPSK has a much higher spectral containment than non-offset QPSK when transmitted over bandlimited nonlinear channels. As a compromise between these two spectral efficiencies, $\pi/4$-DQPSK was proposed (see [13] for the original introduction of this modulation method), whose detection can be performed by a straightforward modification of the techniques used for conventional DQPSK and also for multiple-symbol detection of DQPSK [14]. While $\pi/4$-DQPSK offered a modest improvement in spectral containment over QPSK (the maximum instantaneous phase transitions are reduced from 180 deg for the latter to 135 deg for the former) at little or no sacrifice in power efficiency, it was still a far cry from the spectral efficiency achieved by OQPSK. Understanding that, because of the inherent crosstalk between quadrature channels introduced by the lack of absolute phase knowledge associated with differential detection, one would expect to pay a power

[1] Communications Systems and Research Section.

The research described in this publication was carried out by the Jet Propulsion Laboratory, California Institute of Technology, under a contract with the National Aeronautics and Space Administration.

penalty when differentially detecting OQPSK (DOQPSK), the author set out to find the "best" one could do in this regard. Specifically, by applying the same MLSE principle used to achieve the performance enhancement of DQPSK attained in [1], we derive an analogous multiple-observation interval differential detection technique for OQPSK and examine its behavior in the limit of a large observation time.

In what follows, we start by identifying an equivalent precoded continuous phase modulation (CPM) structure first for OQPSK and then next for differentially encoded OQPSK. It is shown that the required precoding for this equivalence is such as to result in a *ternary* (0,−1,+1) CPM input alphabet.[2] Following this, we recall the results of the author for ML block detection of noncoherent CPM reported in [15] and then apply the technique used there to derive the decision metric and associated receiver structure for the precoded version that equivalently represents differentially encoded OQPSK. Finally, we evaluate (in terms of upper bounds) the average bit-error probability performance of this multiple-bit DOQPSK scheme for cases of practical interest and compare it with the analogous results for non-offset QPSK.

II. Precoded CPM Equivalent of OQPSK and Differentially Encoded OQPSK

In this section, we describe a representation of conventional OQPSK (rectangular pulse shaping implied) in the form of a precoded CPM modulation. Specifically, OQPSK has the form

$$s(t) = \sqrt{\frac{2E_b}{T_b}} \cos\left(2\pi f_c t + \phi\left(t, \boldsymbol{\alpha}\right) + \phi_0\right), \quad nT_b \le t \le (n+1)T_b \tag{1}$$

where E_b and T_b respectively denote the energy and duration of a bit ($P = E_b/T_b$ is the signal power), and f_c is the carrier frequency. In addition, $\phi\left(t, \boldsymbol{\alpha}\right)$ is the phase modulation process that is expressible in the form

$$\phi\left(t, \boldsymbol{\alpha}\right) = \pi \sum_{i \le n} \alpha_i q\left(t - iT_b\right) \tag{2}$$

where $\boldsymbol{\alpha} = (\cdots, \alpha_{-2}, \alpha_{-1}, \alpha_0, \alpha_1, \alpha_2, \cdots)$ is a precoded version of the true data sequence and $q(t)$ is the normalized phase-smoothing response that defines how the underlying phase, $\pi\alpha_i$, evolves with time during the associated bit interval. Without loss of generality, the arbitrary phase constant, ϕ_0, can be set to zero. For OQPSK, the phase pulse $q(t)$ is a step function, i.e., $q\left(t\right) = \left(1/2\right) u\left(t\right)$ [equivalently, the frequency pulse $g\left(t\right) = dq\left(t\right)/dt$ is the impulse function $g\left(t\right) = \left(1/2\right)\delta\left(t\right)$] and the ith element of the CPM data sequence, α_i, can be shown to be related to the true input data bit sequence $\mathbf{a} = (\cdots, a_{-2}, a_{-1}, a_0, a_1, a_2, \cdots)$ by [17, Chap. 3, pp. 177–178][3]

$$\alpha_i = (-1)^{i+1} \frac{a_{i-1}\left(a_i - a_{i-2}\right)}{2} \tag{3}$$

Since the a_i's take on ± 1 values, then the α_i's come from a ternary (−1,0,+1) alphabet. However, in any given bit (half-symbol) interval, the α_i's can assume only one of two equiprobable values, namely, 0 and +1 or 0 and −1, with the further restriction that a +1 cannot be followed by a −1, or vice versa. Thus, in reality, the modulation scheme is a binary CPM but one whose data alphabet can vary (between

[2] As we shall see, the alphabet in any given bit interval is actually binary; however, depending on the data sequence, it varies from bit to bit between (0,−1) and (0,+1).

[3] Note that the in-phase (I) and quadrature-phase (Q) data symbols of the I-Q representation of OQPSK are respectively obtained as the even and odd bits of the sequence **a**. Also note that, whereas this representation contains I and Q data sequences at the symbol rate, the effective data sequence for the CPM representation occurs at the half-symbol (bit) rate.

two choices) from bit interval to bit interval. Another way of characterizing the variation rule for the data alphabet is as follows: If the previous bit is 0, then the data alphabet for the current bit is switched relative to that available for the previous bit, i.e., if it was (0,+1) for the previous transmission, it becomes (0,−1) for the current transmission, and vice versa. On the other hand, if the previous bit is a +1 or a −1, then the data alphabet for the current bit remains the same as that available for the previous bit, e.g., if it was (0,+1) for the previous transmission, it is again (0,+1) for the current transmission.

In view of the representation in Eq. (2), we see that a value of $\alpha_i = 0$ suggests no change in carrier phase [no transition occurs in the I (or Q) data symbol sequence at the midsymbol time instant of the Q (I) data symbol], whereas a value of $\alpha_i = \pm 1$ suggests a carrier phase change of $\pm\pi/2$ [a transition occurs in the I (or Q) data symbol sequence at the midsymbol time instant of the Q (I) data symbol]. Finally, note that since the duration of the frequency pulse does not exceed the baud (bit) interval, then the CPM representation of OQPSK is full response and can be implemented with the cascade of a precoder satisfying Eq. (3) and a conventional CPM modulator (see Fig. 1).

In order to find a precoded CPM representation for differentially encoded OQPSK, we recall that if $\{b_n\}$ is a binary (± 1) independent and identically distributed (i.i.d.) sequence, then $\{a_n\}$ with elements $a_n = b_n a_{n-1}$ is the differentially encoded version of $\{b_n\}$ and is also i.i.d. Alternatively, since $b_n = a_n a_{n-1}$, then the precoder of Eq. (3) can be rewritten in terms of the b_n's as

$$\alpha_i = (-1)^{i+1} \frac{b_i - b_{i-1}}{2} \tag{4}$$

Thus, Fig. 1 is also a precoded CPM representation of differentially encoded OQPSK if the precoder of Eq. (4) is used instead of that in Eq. (3). It is important to note that while for either OQPSK or differentially encoded OQPSK the input data sequence is i.i.d., the data sequence input to the CPM modulator, namely, $\{\alpha_n\}$, is not i.i.d. In particular, it is straightforward to show from Eq. (4) that

$$E\{\alpha_n \alpha_{n-m}\} = \begin{cases} \frac{1}{4}, & |m| = 1 \\ \frac{1}{2}, & m = 0 \\ 0, & \text{otherwise} \end{cases} \tag{5}$$

Thus, we see from Eq. (5) that adjacent symbols are correlated. Furthermore, the a priori probabilities of the α_n's are given by

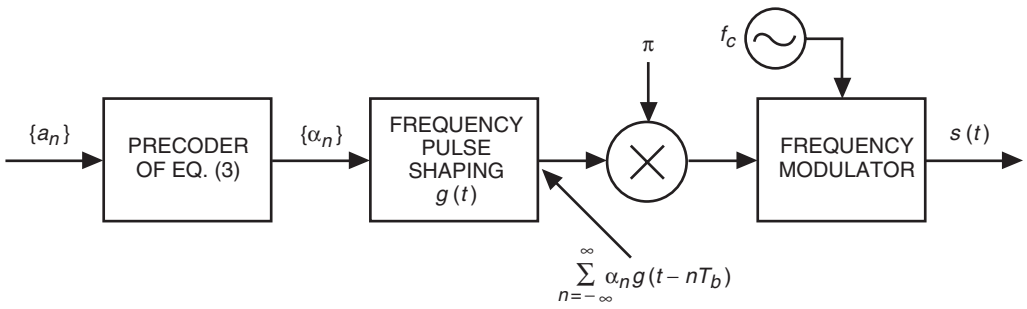

Fig. 1. Precoded CPM transmitter equivalent to OQPSK.

$$\Pr\{\alpha_n = d\} = \begin{cases} \dfrac{1}{4}, & |d| = 1 \\ \dfrac{1}{2}, & d = 0 \end{cases} \tag{6}$$

and the first-order conditional probabilities are given by

$$\left.\begin{aligned} \Pr\{\alpha_n = 0 \,|\alpha_{n-1} = 0\} &= \frac{1}{2} \\ \Pr\{\alpha_n = 1 \,|\alpha_{n-1} = 0\} &= \Pr\{\alpha_n = -1 \,|\alpha_{n-1} = 0\} = \frac{1}{4} \\ \Pr\{\alpha_n = 0 \,|\alpha_{n-1} = 1\} &= \Pr\{\alpha_n = 0 \,|\alpha_{n-1} = -1\} = \frac{1}{2} \\ \Pr\{\alpha_n = 1 \,|\alpha_{n-1} = 1\} &= \Pr\{\alpha_n = -1 \,|\alpha_{n-1} = -1\} = \frac{1}{2} \\ \Pr\{\alpha_n = 1 \,|\alpha_{n-1} = -1\} &= \Pr\{\alpha_n = -1 \,|\alpha_{n-1} = 1\} = 0 \end{aligned}\right\} \tag{7}$$

Since the noncoherent demodulator of the CPM modulation will result in decisions $\{\hat{\alpha}_n\}$ on the symbols $\{\alpha_n\}$, then in order to convert these decisions into ones on the true input binary data sequence ($\{b_n\}$ for differentially encoded OQPSK), one would have to follow the CPM demodulator with a decoder that reverses the precoding operation in Eq. (4). Rather than do that, one can include an additional differential encoding operation at the transmitter in such a way that the decisions $\{\hat{\alpha}_n\}$ on the symbols $\{\alpha_n\}$ will now directly reflect decisions on the true binary data input. To see how this can be accomplished, we define

$$c_n = 1 - 2\,|\alpha_n| = 1 - |b_n - b_{n-1}| \tag{8}$$

Thus, $c_n = -1$ if b_{n-1} makes a transition and $c_n = 1$ if b_{n-1} does not make a transition. Since the relation between c_n and b_n is again that of conventional differential encoding, we see that decisions $\{\hat{c}_n\}$ derived from the CPM demodulator decisions $\{\hat{\alpha}_n\}$ in accordance with Eq. (8) will represent decisions on an input data sequence $\{c_n\}$ whose differentially encoded version is $\{b_n\}$. The inclusion of this additional differential encoder at the input of the OQPSK modulator results in a transmitter that implements OQPSK with a *double* differential encoder of its input binary data sequence (see Fig. 2 for the complete system).[4] However, it can be shown that double differentially encoding the binary input sequence prior to demultiplexing into in-phase (I) and quadrature-phase (Q) sequences is exactly equivalent to first demultiplexing the input sequence and then differentially encoding the binary I and Q symbols [each of duration $2T_b$ and offset with respect to one another (see Fig. 3)]. Since differentially encoded OQPSK normally is implemented as in Fig. 3, then the CPM receiver of Fig. 2 is, in reality, an appropriate demodulator of what is conventionally known as differentially encoded OQPSK. Before concluding, we note that the "folding over" of the three-level α_n decisions into two-level c_n decisions in accordance with Eq. (8) is analogous to what takes place in the decision rule for duobinary modulation [16, pp. 569–575].

[4] Note that double differential encoding a binary input sequence of rate $1/T_b$ is equivalent to passing the same sequence through a single differential encoder having a delay of $2T_b$ [16, Chap. 8].

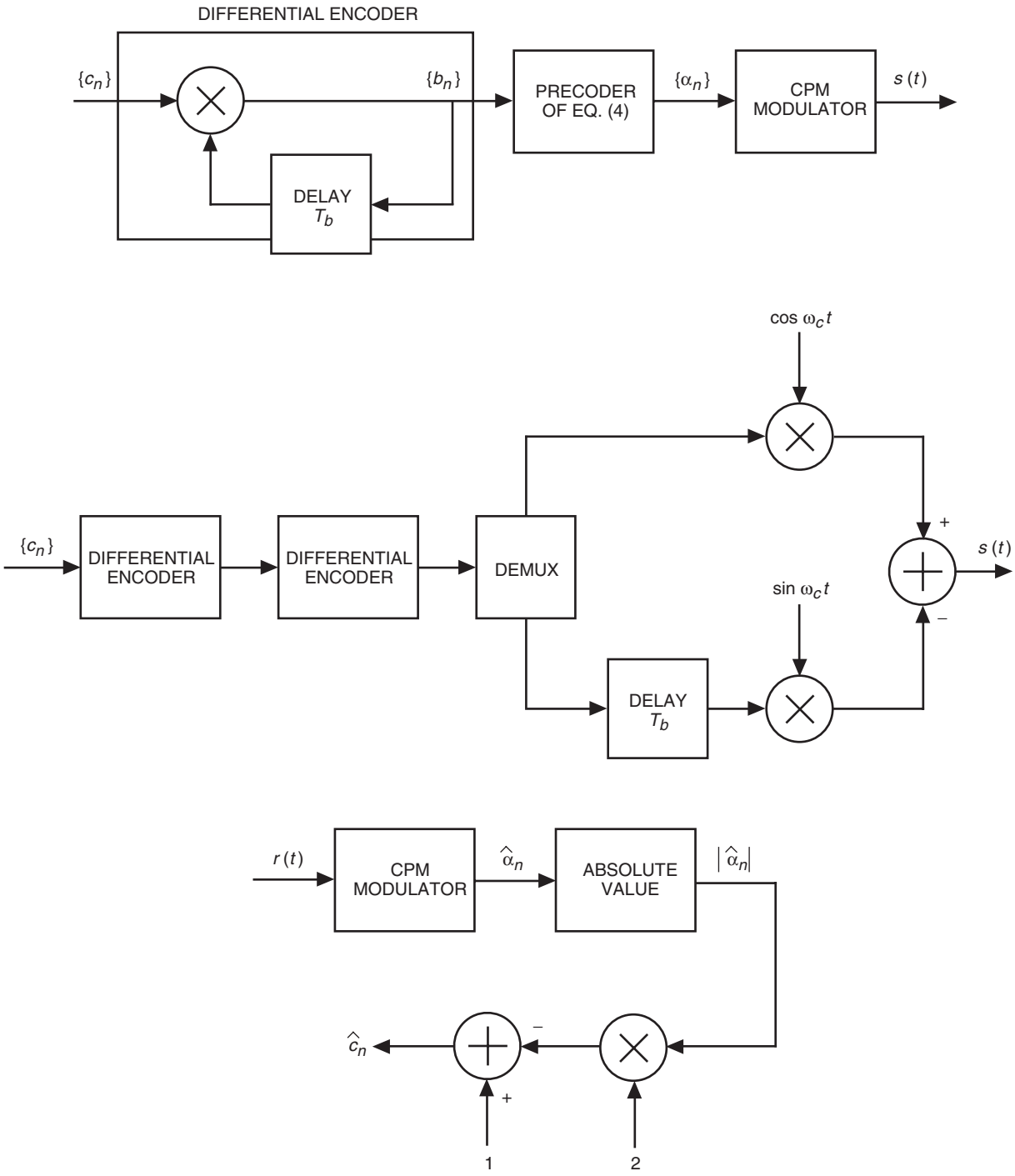

Fig. 2. Equivalent precoded CPM and OQPSK with double differentially encoded binary input stream transmitters and also a noncoherent CPM demodulator.

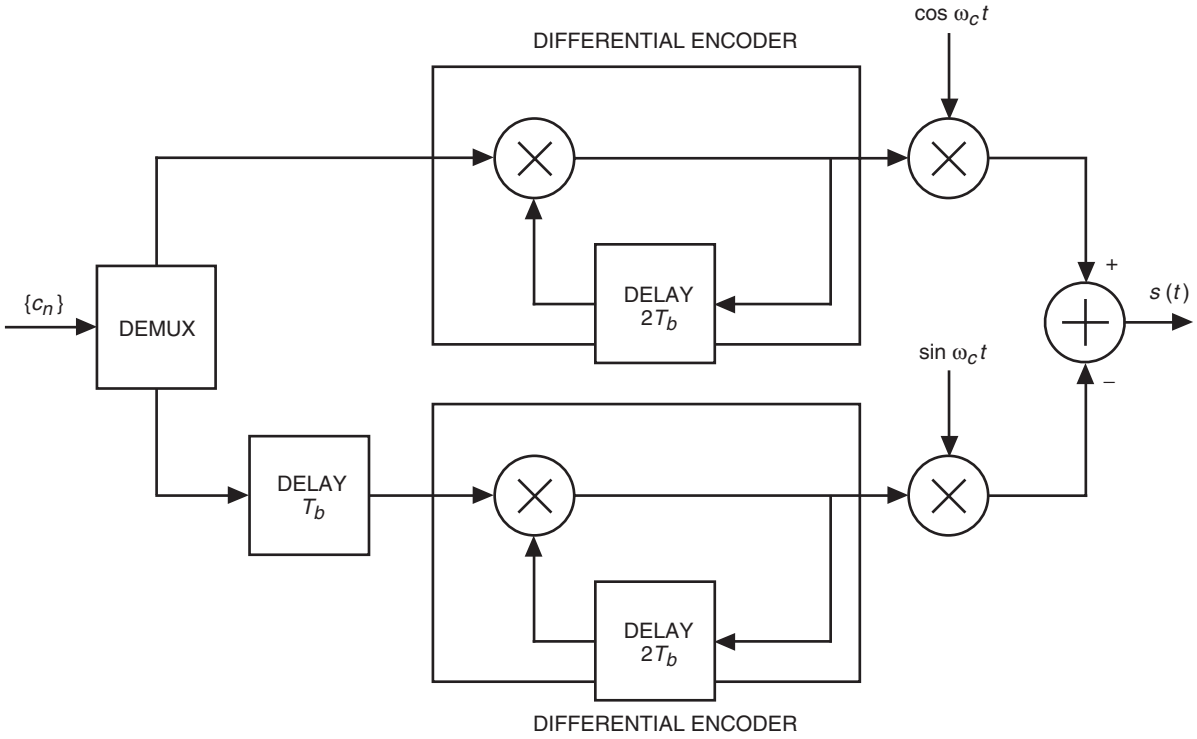

Fig. 3. Differentially encoded OQPSK transmitter equivalent to OQPSK with the double differentially encoded binary input stream transmitter of Fig. 2.

III. Maximum-Likelihood Sequence Detection of Noncoherent Precoded CPM

Expressing the real signal of Eq. (1) in complex baseband form, i.e., $s(t) = \mathrm{Re}\left\{\tilde{S}(t)\, e^{j\omega_c t}\right\}$, where $\tilde{S}(t) = \sqrt{2E_b/T_b}e^{j\phi(t,\boldsymbol{\alpha})}$, then transmitting $\tilde{S}(t)$ over an additive white Gaussian noise (AWGN) channel results in a received complex baseband signal $\tilde{R}(t)$ of the form

$$\tilde{R}(t) = \tilde{S}(t)\, e^{j\theta(t)} + n(t) \tag{9}$$

where $n(t)$ is a zero-mean complex Gaussian noise process with two-sided power spectral density $2N_0$ W/Hz and $\theta(t)$ is an arbitrary phase introduced by the channel, which is assumed to be constant (independent of time) over some specified interval of time, i.e., $\theta(t) = \theta$, but is otherwise unknown. Furthermore, in the absence of any side information, θ is assumed to be uniformly distributed in the interval $(-\pi, \pi)$. Following the approach taken in [15], for an N-bit observation, the MLSE decision rule for jointly detecting the data sequence $\boldsymbol{\alpha} = \alpha_{n-N+1}, \alpha_{n-N+2}, \cdots, \alpha_{n-1}, \alpha_n$ is given by[5]

$$\text{Choose } \boldsymbol{\alpha} = \boldsymbol{\alpha}^* \text{ corresponding to } |\beta(\boldsymbol{\alpha}^*)| = \max_{a} |\beta(\boldsymbol{\alpha})| \tag{10}$$

where[6]

[5] The notation $\boldsymbol{\alpha}^*$ is intended to denote a particular sequence $\boldsymbol{\alpha}$, not its complex conjugate.

[6] Note that the definitions of Γ_n and C_n are slightly different from those in [15]; however, the product $\Gamma_n C_n$ remains unchanged.

$$\beta(\boldsymbol{\alpha}) = \sum_{l=0}^{N-1} \Gamma_{n-l} C_{n-l} \tag{11}$$

with

$$\Gamma_n = \int_{nT_b}^{(n+1)T_b} \tilde{R}(t)\, dt \tag{12}$$

representing the observation corresponding to the nth bit interval, i.e., the complex output of an integrate-and-dump (I&D) filter and the coefficients $\{C_n\}$ defined recursively by

$$C_{n-l} = e^{-j(\pi/2)\alpha_{n-l}} C_{n-l-1},\ l = 0, 1, \cdots, N-2, \quad C_{n-N+1} = e^{-j(\pi/2)\alpha_{n-N+1}} \tag{13}$$

The corresponding phase trellis is illustrated in Fig. 4.[7] Since the decision rule in Eq. (10) involves only the magnitude of $\beta(\boldsymbol{\alpha})$, then noting that the factor $\exp[-j(\pi/2)\alpha_{n-N+1}]$ is common to each term of the sum in Eq. (11), we obtain

$$|\beta(\boldsymbol{\alpha})| = \left| \sum_{l=0}^{N-1} \Gamma_{n-l} \exp\left(-j\frac{\pi}{2} \sum_{k=l}^{N-2} \alpha_{n-k} \right) \right| = \left| \sum_{l=0}^{N-1} \Gamma_{n-l}\, j^{-\sum_{k=l}^{N-2} \alpha_{n-k}} \right| \tag{14}$$

Thus, we observe from Eq. (14) that an observation of N bits actually results in a decision on only the $N-1$ most recent bits, $\alpha_{n-N+2}, \cdots, \alpha_{n-1}, \alpha_n$, as was the case for the multiple-symbol differential detection scheme described in [1]. Equivalently, to perform block-by-block detection, the observation intervals must be overlapped by one bit, i.e., the one that serves as a reference for detecting the remaining $N-1$ bits. Finally, to arrive at decisions on the true input data stream, $\{c_n\}$, the decision rule of Eq. (10) is modified in accordance with Eq. (8) to become

$$\text{Choose } \mathbf{c} = \mathbf{c}^* = 1 - 2|\boldsymbol{\alpha}^*| \text{ corresponding to } |\beta(\boldsymbol{\alpha}^*)| = \max_a |\beta(\boldsymbol{\alpha})| \tag{15}$$

Using recursive techniques, it can be shown that the number of values over which $|\beta(\boldsymbol{\alpha})|$ is to be maximized, or, equivalently, the number of possible sequences $\alpha_{n-N+2}, \cdots, \alpha_{n-1}, \alpha_n$ of length $N-1$ is given by

$$N_s = 5 \sum_{k=0}^{\lfloor \frac{N-2}{2} \rfloor} \binom{N-2}{2k} 2^k + 2 \sum_{k=0}^{\lfloor \frac{N-3}{2} \rfloor} \binom{N-3}{2k} 2^k \tag{16}$$

Before concluding this section, we note that had we simply input a binary i.i.d. data sequence directly [without the precoding of Eq. (3) or Eq. (4)] into the CPM modulator of Fig. 1, then the resulting output would be a binary PSK (BPSK) signal. Alternatively, if a conventional differential encoder were used as

[7] For the purpose of clarity, a narrow frequency pulse is assumed rather than an impulse.

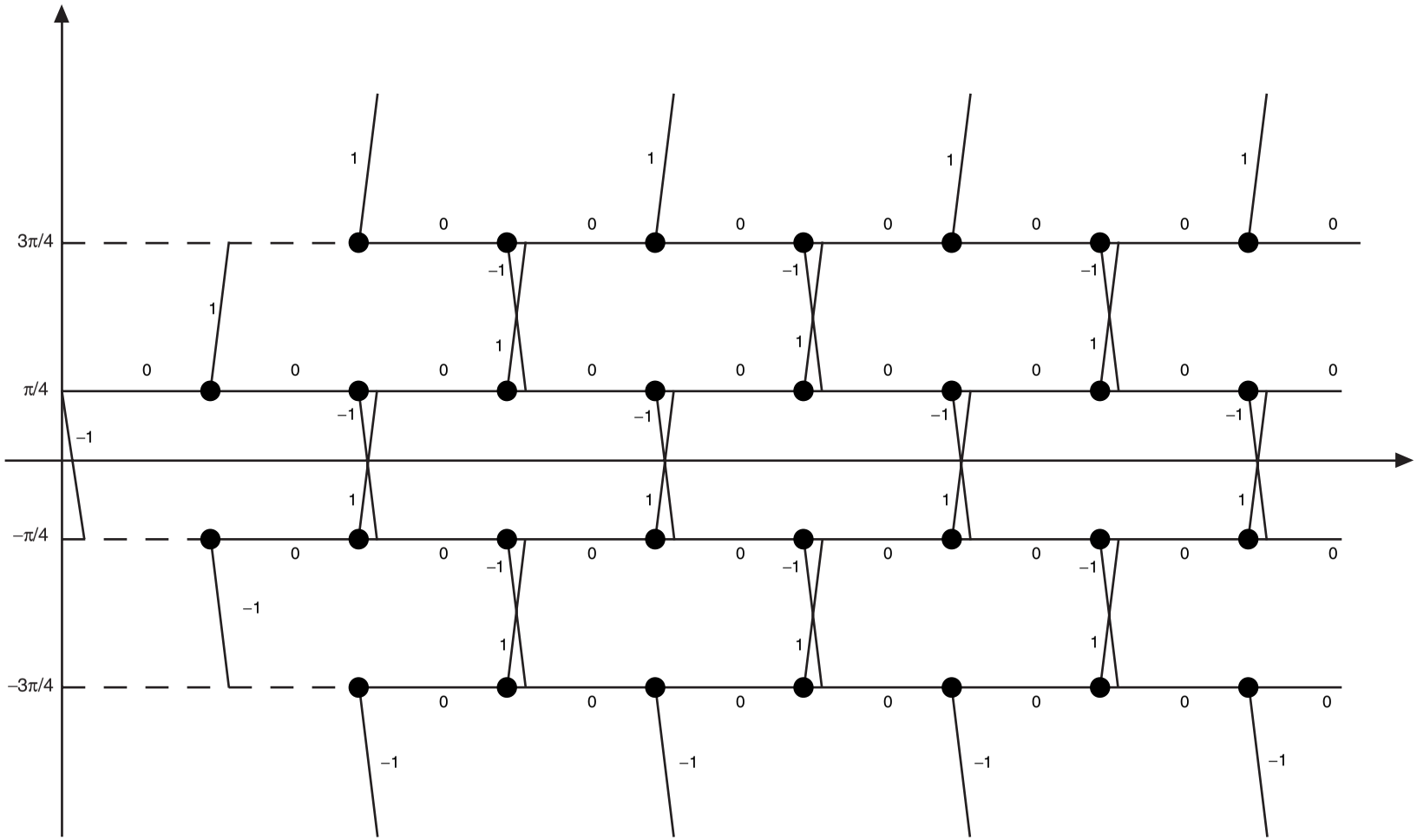

Fig. 4. Phase trellis diagram for OQPSK (branches are labeled with values of α_i).

the precoder, then the output would be differentially encoded BPSK. In the case of the latter, the decision rule of Eq. (10) combined with Eqs. (11) and (12) would precisely result in multiple-bit differential detection of BPSK, as one might expect. The difference here is that for OQPSK the alphabet from which the α_n's are chosen is ternary (in the sense explained above) and pairwise correlated as opposed to BPSK, where it is purely binary and i.i.d.

To illustrate the above, let us consider a simple example corresponding to $N = 3$. For this case, we obtain the following decision rule:

$$\text{Choose } c_{n-1}^* = 1 - 2\left|\alpha_{n-1}^*\right| \text{ and } c_n^* = 1 - 2\left|\alpha_n^*\right| \text{ corresponding to}$$

$$\max_{\alpha_{n-1},\alpha_n} \left|\Gamma_{n-2} + j^{-\alpha_{n-1}}\Gamma_{n-1} + j^{-(\alpha_{n-1}+\alpha_n)}\Gamma_n\right| \tag{17}$$

The $N_s = 7$ possible values of $|\beta(\alpha_{n-1}, \alpha_n)|$ corresponding to Eq. (17) and their associated correct decisions, c_{n-1}^* and c_n^*, are

α_{n-1}	α_n	$\lvert\beta(\alpha_{n-1},\alpha_n)\rvert$	c_{n-1}^*	c_n^*
0	0	$\lvert\Gamma_{n-2} + \Gamma_{n-1} + \Gamma_n\rvert$	1	1
0	1	$\lvert\Gamma_{n-2} + \Gamma_{n-1} - j\Gamma_n\rvert$	1	−1
0	−1	$\lvert\Gamma_{n-2} + \Gamma_{n-1} + j\Gamma_n\rvert$	1	−1
1	0	$\lvert\Gamma_{n-2} - j\Gamma_{n-1} - j\Gamma_n\rvert$	−1	1
−1	0	$\lvert\Gamma_{n-2} + j\Gamma_{n-1} + j\Gamma_n\rvert$	−1	1
1	1	$\lvert\Gamma_{n-2} - j\Gamma_{n-1} - \Gamma_n\rvert$	−1	−1
−1	−1	$\lvert\Gamma_{n-2} + j\Gamma_{n-1} - \Gamma_n\rvert$	−1	−1

(18)

which are all unique. Note from Eqs. (6) and (7) that the a priori joint probabilities of the combinations of transmitted pairs α_{n-1}, α_n corresponding to each of the four possible decision pairs c_{n-1}^*, c_n^* are all equal to 1/4.

IV. Evaluation of an Upper Bound on Average Bit-Error Probability

To evaluate the performance of the receiver in Fig. 2, we make use of the technique in [1] to obtain an upper bound on the average bit-error probability (BEP). In particular, we use a union bound analogous to that used for upper bounding the performance of error-correction-coded systems. This bound is expressed as the sum of the pairwise error probabilities (PEPs) associated with each N-bit error block. For our case, the PEPs can be evaluated exactly using the results of Stein [18] as applied to the noncoherent CPM problem in [19].

Mathematically speaking, let $\mathbf{c} = (c_{n-N+2}, c_{n-N+3}, \cdots, c_{n-1}, c_n)$ denote the sequence of $N-1$ information bits and $\hat{\mathbf{c}} = (\hat{c}_{n-N+2}, \hat{c}_{n-N+3}, \cdots, \hat{c}_{n-1}, \hat{c}_n)$ be the corresponding sequence of detected bits. Then,

$$P_b(E) \leq \frac{1}{N-1}\frac{1}{2^{N-1}} \sum_{\mathbf{c}} \sum_{\hat{\mathbf{c}} \neq \mathbf{c}} w(\mathbf{c}, \hat{\mathbf{c}}) P(\mathbf{c}, \hat{\mathbf{c}}) \Pr\left\{\left|\hat{\beta}\right| > |\beta| \| \mathbf{c}\right\} \tag{19}$$

where $w(\mathbf{c}, \hat{\mathbf{c}})$ denotes the Hamming distance between $\mathbf{c}$ and $\hat{\mathbf{c}}$ (i.e., the number of bits in which they disagree), $\Pr\left\{\left|\hat{\beta}\right| > |\beta| \| \mathbf{c}\right\}$ denotes the PEP that $\hat{\mathbf{c}}$ is chosen when $\mathbf{c}$ is sent, and $P(\mathbf{c}, \hat{\mathbf{c}}) = 1/N_e(\mathbf{c}, \hat{\mathbf{c}})$, where $N_e(\mathbf{c}, \hat{\mathbf{c}})$ is the number of different error sequence pairs that have to be considered for a particular $(\mathbf{c}, \hat{\mathbf{c}})$.[8] Note that $\sum_{\mathbf{c}} \sum_{\hat{\mathbf{c}} \neq \mathbf{c}} P(\mathbf{c}, \hat{\mathbf{c}}) = 2^{N-1}\left(2^{N-1} - 1\right)$. The decision statistic $|\beta|$ is defined in Eq. (14) and $\left|\hat{\beta}\right|$ is identical to Eq. (14) with $\mathbf{c}$ (or equivalently $\boldsymbol{\alpha}$) replaced by $\hat{\mathbf{c}}$ (or equivalently $\hat{\boldsymbol{\alpha}}$). Note that the number of PEPs, $\Pr\left\{\left|\hat{\beta}\right| > |\beta| \| \mathbf{c}\right\}$, for any particular true sequence $\mathbf{c}$ depends on the sequence itself. For example, we see from Eq. (18) that, for $N = 3$, there are six PEPs corresponding to $\mathbf{c} = (1, 1)$, whereas for each of the remaining three $\mathbf{c}$ sequences, namely, $(1, -1), (-1, 1)$, and $(-1, -1)$, there are two groups of five PEPs.

A. Evaluation of the Pairwise Error Probability

To compute $\Pr\left\{\left|\hat{\beta}\right| > |\beta| \| \mathbf{c}\right\}$ or, equivalently, $\Pr\left\{\left|\hat{\beta}\right|^2 > |\beta|^2 | \mathbf{c}\right\}$, we use the approach taken in [15], which is in turn based on the approach used in [18] to evaluate the performance of noncoherent FSK. Specifically, letting $\eta = |\beta|^2$ and $\hat{\eta} = \left|\hat{\beta}\right|^2$, then

$$\Pr\{\hat{\eta} > \eta | \mathbf{c}\} = \frac{1}{2}\left[1 - Q\left(\sqrt{b}, \sqrt{a}\right) + Q\left(\sqrt{a}, \sqrt{b}\right)\right] \tag{20}$$

where $Q(a, b)$ is the first-order Marcum Q-function [20] and

$$\left\{\begin{matrix} b \\ a \end{matrix}\right\} = \frac{E_b}{2N_0}\left(N \pm \sqrt{N^2 - |\delta|^2}\right) \tag{21}$$

with E_b/N_0 denoting the bit signal-to-noise ratio (SNR) and

$$\delta \triangleq \sum_{l=0}^{N-1} j \sum_{m=0}^{N-l-2} (\alpha_{n-l-m} - \hat{\alpha}_{n-l-m}) = \sum_{l=0}^{N-1} j \sum_{m=0}^{N-l-2} \Delta\alpha_{n-l-m} \tag{22}$$

It is understood that the summation in the exponent evaluates to zero if the upper index is negative.

---

[8] Note that, for the analogous M-DQPSK problem considered in [1], $N_e(\mathbf{c}, \hat{\mathbf{c}}) = 1$ for all $\mathbf{c}$ and $\hat{\mathbf{c}}$, and thus the term $P(\mathbf{c}, \hat{\mathbf{c}})$ was absent in the union bound on BEP.

B. Case I: $N = 2$

To illustrate the procedure, consider the simplest case corresponding to $N = 2$. Tabulated below are the possible error sequences and corresponding values of $|\delta|^2$, $P(\mathbf{c}, \hat{\mathbf{c}})$, and $w(\mathbf{c}, \hat{\mathbf{c}})$:

α_n	$\hat{\alpha}_n$	$\Delta\alpha_n$	$\lvert\delta\rvert^2 = \lvert 1 + j^{\Delta\alpha_n}\rvert^2$	c_n	$\hat{c}_n$	$w(\mathbf{c}, \hat{\mathbf{c}})$	$P(\mathbf{c}, \hat{\mathbf{c}})$
0	1	−1	2	1	−1	1	1/2
0	−1	1	2	1	−1	1	1/2
1	0	1	2	−1	1	1	1/2
−1	0	−1	2	−1	1	1	1/2

(23)

Thus, since there is only one value of $|\delta|^2$ for all the error sequences, there is only one PEP type that is evaluated from Eqs. (20) and (21) as

$$\text{PEP} = \frac{1}{2}\left[1 - Q\left(\sqrt{\frac{E_b}{2N_0}\left(2+\sqrt{2}\right)}, \sqrt{\frac{E_b}{2N_0}\left(2-\sqrt{2}\right)}\right) + Q\left(\sqrt{\frac{E_b}{2N_0}\left(2-\sqrt{2}\right)}, \sqrt{\frac{E_b}{2N_0}\left(2+\sqrt{2}\right)}\right)\right] \tag{24}$$

Finally, using the values of $w(\mathbf{c}, \hat{\mathbf{c}})$ and $P(\mathbf{c}, \hat{\mathbf{c}})$ from the above table, we obtain the upper bound on average BEP from Eq. (19) as

$$P_b(E) \leq \frac{1}{2}\left[1 - Q\left(\sqrt{\frac{E_b}{2N_0}\left(2+\sqrt{2}\right)}, \sqrt{\frac{E_b}{2N_0}\left(2-\sqrt{2}\right)}\right) + Q\left(\sqrt{\frac{E_b}{2N_0}\left(2-\sqrt{2}\right)}, \sqrt{\frac{E_b}{2N_0}\left(2+\sqrt{2}\right)}\right)\right] \tag{25}$$

Comparing Eq. (25) with the optimum average BEP performance of DQPSK (which is exactly given by the right-hand side of Eq. (25) with E_b replaced by $E_s = 2E_b$), we note that, for a two-bit observation interval, the performance of the DOQPSK receiver is at most 3 dB worse (based on the upper bound). In fact, it is not difficult to show that the upper bound of Eq. (25) is in fact equal to the actual average BEP performance of the DOQPSK receiver and thus the penalty relative to DQPSK is *exactly* 3 dB. This should not at all be surprising since the optimum DQPSK receiver [16, Chap. 7] makes differential decisions based on an observation of two *symbol* intervals (four bit intervals), whereas the DOQPSK receiver makes differential decisions based on an observation of two *bit* intervals.

C. Case II: $N = 3$

To further illustrate the procedure, consider once again the $N = 3$ case previously introduced in Section III. For this case, it can be shown that there are a total of 36 possible error sequence pairs resulting in only two different values of $|\delta|^2$, namely, $|\delta|^2 = 1$ and $|\delta|^2 = 5$, corresponding respectively to $b = 3 + 2\sqrt{2},\ a = 3 - 2\sqrt{2}$ and $b = 5, a = 1$. The corresponding PEP types in accordance with Eq. (20) are then

$$\mathrm{PEP}_1 = \frac{1}{2}\left[1 - Q\left(\sqrt{\frac{E_b}{N_0}\left(\frac{3}{2}+\sqrt{2}\right)}, \sqrt{\frac{E_b}{N_0}\left(\frac{3}{2}-\sqrt{2}\right)}\right) + Q\left(\sqrt{\frac{E_b}{N_0}\left(\frac{3}{2}-\sqrt{2}\right)}, \sqrt{\frac{E_b}{N_0}\left(\frac{3}{2}+\sqrt{2}\right)}\right)\right]$$

$$\mathrm{PEP}_2 = \frac{1}{2}\left[1 - Q\left(\sqrt{\frac{5E_b}{2N_0}}, \sqrt{\frac{E_b}{2N_0}}\right) + Q\left(\sqrt{\frac{E_b}{2N_0}}, \sqrt{\frac{5E_b}{2N_0}}\right)\right] \tag{26}$$

The accumulated value of $w(\mathbf{c}, \hat{\mathbf{c}})\, P(\mathbf{c}, \hat{\mathbf{c}})$ for both of these PEPs is $w(\mathbf{c}, \hat{\mathbf{c}})\, P(\mathbf{c}, \hat{\mathbf{c}}) = 8$. Finally then, the upper bound on the average BEP of Eq. (19) is given by

$$P_b(E) \leq \mathrm{PEP}_1 + \mathrm{PEP}_2 \tag{27}$$

D. Asymptotic Behavior

It is of interest to examine the asymptotic behavior of the average BEP in the limit of large E_b/N_0 so as to determine the amount of "coding gain"[9] achieved as a function of the length of the observation interval. Borrowing a result from [1], in the limit of large SNR, the PEP of Eq. (20) can be approximated by

$$\Pr\{\hat{\eta} > \eta \,|\mathbf{c}\} \cong \frac{1}{2\sqrt{\pi E_b/N_0}} \sqrt{\frac{N+|\delta|}{|\delta|\,(N-|\delta|)}} \exp\left\{-\frac{E_b}{2N_0}\,(N-|\delta|)\right\} \tag{28}$$

or, using the asymptotic expansion for the complementary error function, i.e.,

$$\operatorname{erfc} x \cong \frac{1}{\sqrt{\pi}x} \exp\left(-x^2\right) \tag{29}$$

Eq. (28) becomes

$$\Pr\{\hat{\eta} > \eta \,|\mathbf{c}\} \cong \sqrt{\frac{N+|\delta|}{8\,|\delta|}} \operatorname{erfc}\left(\sqrt{\frac{E_b}{2N_0}\,(N-|\delta|)}\right) \tag{30}$$

For $N = 2$, we observed that $|\delta| = \sqrt{2}$ for all four of the error sequence pairs. Thus, the PEP, or equivalently, the average BEP, can be asymptotically upper bounded (approximated) by

$$P_b(E) \lesssim \frac{1}{2}\sqrt{\frac{1+\sqrt{2}}{2}} \operatorname{erfc}\left(\sqrt{\frac{E_b}{N_0}\left(\frac{2-\sqrt{2}}{2}\right)}\right) \tag{31}$$

which, ignoring the factor preceding the complementary error function, performs $-10\log_{10}\left(1-1/\sqrt{2}\right) = 5.33$ dB worse than *coherent* detection of differentially encoded QPSK [16, Chap. 4].

For $N = 3$, applying the approximation of Eq. (30) to the two PEPs in Eq. (26) gives

[9] By "coding gain" is meant the asymptotic reduction in required E_b/N_0 (based on the upper bound) that results from an MLSE based on an N-bit observation as opposed to a two-bit observation.

$$\left.\begin{aligned} \mathrm{PEP}_1 &\cong \frac{1}{\sqrt{2}}\,\mathrm{erfc}\left(\sqrt{\frac{E_b}{N_0}}\right) \\ \mathrm{PEP}_2 &\cong \frac{1}{2}\sqrt{\frac{3+\sqrt{5}}{2\sqrt{5}}}\,\mathrm{erfc}\left(\sqrt{\frac{E_b}{N_0}\left(\frac{3-\sqrt{5}}{2}\right)}\right) \end{aligned}\right\} \tag{32}$$

Since, for large SNR, PEP_2 dominates over PEP_1, then the average PEP is asymptotically upper bounded by

$$P_b(E) \lesssim \frac{1}{2}\sqrt{\frac{3+\sqrt{5}}{2\sqrt{5}}}\,\mathrm{erfc}\left(\sqrt{\frac{E_b}{N_0}\left(\frac{3-\sqrt{5}}{2}\right)}\right) \tag{33}$$

which, ignoring the factor preceding the complementary error function, represents an improvement of $10\log_{10}\left[\left(3-\sqrt{5}\right)/\left(2-\sqrt{2}\right)\right] = 1.153$ dB over the two-bit observation case.

E. General Asymptotic Behavior

Analogous to what was observed in the previous subsection, in the general case of arbitrary N, the dominant terms in the average BEP occur for the sequences that result in the minimum value of $N-|\delta|$, or, equivalently, the maximum value of $|\delta|$. One can easily show that this minimum value will certainly occur for the error sequence $\hat{\boldsymbol{\alpha}}$ having $N-1$ elements equal to the correct sequence $\boldsymbol{\alpha}$ and one element with the smallest error. Thus, as in [1], either

$$\min_{\boldsymbol{\alpha},\hat{\boldsymbol{\alpha}}}(N-|\delta|) = N - \left|N-1+j^{(\Delta\alpha_n)_{\min}}\right| = N-|N-1\pm j| = N-\sqrt{(N-1)^2+1} \tag{34}$$

or

$$\min_{\boldsymbol{\alpha},\hat{\boldsymbol{\alpha}}}(N-|\delta|) = N - \left|1+(N-1)\,j^{(\Delta\alpha_n)_{\min}}\right| = N-|1\pm(N-1)\,j| = N-\sqrt{(N-1)^2+1} \tag{35}$$

which give identical results for $|\delta|_{\max}$, namely, $|\delta|_{\max} = \sqrt{(N-1)^2+1}$. Hence, in accordance with Eqs. (19) and (30), the average BEP is approximately upper bounded by

$$P_b(E) \lesssim$$

$$\left(\sum_{\mathbf{c}\neq\hat{\mathbf{c}}}\sum w(\mathbf{c},\hat{\mathbf{c}})\,P(\mathbf{c},\hat{\mathbf{c}})\right)\frac{1}{N-1}\,\frac{1}{2^{N-1}}\sqrt{\frac{N+\sqrt{(N-1)^2+1}}{8\sqrt{(N-1)^2+1}}}\,\mathrm{erfc}\left(\sqrt{\frac{E_b}{2N_0}\left(N-\sqrt{(N-1)^2+1}\right)}\right) \tag{36}$$

where the $w(\mathbf{c},\hat{\mathbf{c}})\,P(\mathbf{c},\hat{\mathbf{c}})$ terms in the double summation correspond only to those error sequence pairs that result in $|\delta|_{\max}$. For example, for $N=3$ the term PEP_1 of Eq. (26) corresponds to

$|\delta|_{\max}$ and, as previously stated just below that equation, the accumulated value of $w(\mathbf{c},\hat{\mathbf{c}})\,P(\mathbf{c},\hat{\mathbf{c}})$ is $\sum_{\mathbf{c}\neq\hat{\mathbf{c}}}\sum w(\mathbf{c},\hat{\mathbf{c}})\,P(c,\hat{c}) = 8$. Similarly, for $N = 4$, it can be shown that there are a total of 56 error sequence pairs each of length 3 that result in $|\delta|_{\max}$, and for these sequences $\sum_{\mathbf{c}\neq\hat{\mathbf{c}}}\sum w(\mathbf{c},\hat{\mathbf{c}})\,P(\mathbf{c},\hat{\mathbf{c}}) = 16$. Going one step further, for $N = 5$ there are a total of 152 error sequence pairs each of length 4 that result in $|\delta|_{\max}$, and for these sequences $\sum_{\mathbf{c}\neq\hat{\mathbf{c}}}\sum w(\mathbf{c},\hat{\mathbf{c}})\,P(\mathbf{c},\hat{\mathbf{c}}) = 31.5$.

Figure 5 is an illustration of the asymptotic upper bound on average BEP as computed from Eq. (36) versus E_b/N_0 in dB and parameterized by the sequence length N. As was the case in [1], the largest improvement in performance is obtained for the first few increases in the value of N, with diminishing returns from then on.

Since the "coding gain" is obtained from the argument of the complementary error function, we see that, for arbitrary N, this gain (in dB) is given by

$$G = 10\log_{10}\frac{N - \sqrt{(N-1)^2 + 1}}{2 - \sqrt{2}} \tag{37}$$

Thus, for $N = 4$, the coding gain is 1.554 dB, which therefore represents an asymptotic SNR loss of only 1.446 dB relative to the optimum DQPSK receiver *based on the same observation interval.*[10] In the limit of large N, the coding gain of Eq. (37) becomes

$$\lim_{N\to\infty} G = 10\log_{10}\frac{1}{2 - \sqrt{2}} = 2.323 \tag{38}$$

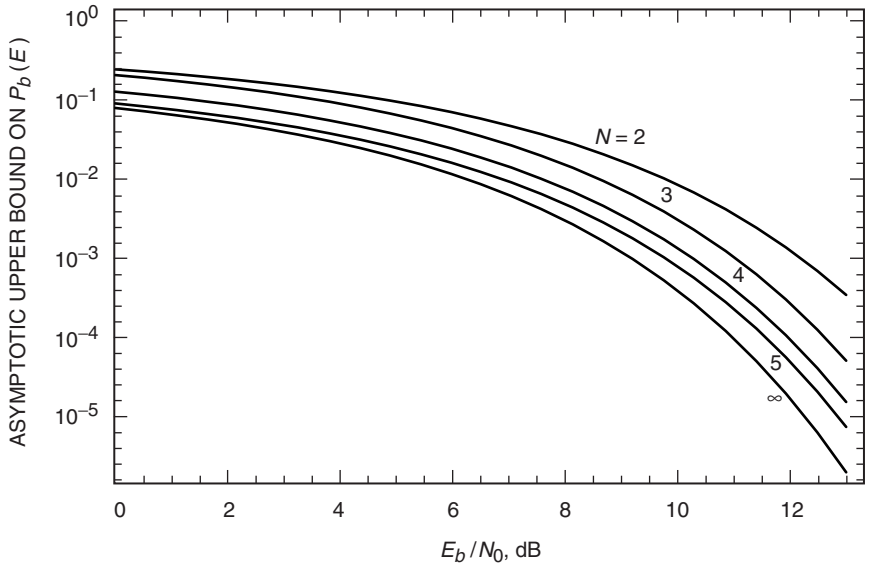

Fig. 5. Asymptotic upper bound on average BEP versus bit energy-to-noise ratio in dB.

[10] Recall that the optimum DQPSK receiver [16, Fig. 7.1] makes its decisions by examining the difference of two symbol decisions, and thus its observation interval is $2T_s = 4T_b$.

which is now only 0.677 dB away from optimum two-symbol observation DQPSK performance. Of course, one can always apply multiple-symbol differential detection to QPSK to also improve its performance, as discussed in [1], which in the limit of large observation time approaches the average BEP performance of *coherent detection* of differentially encoded BPSK (or QPSK). Also, since the asymptotic performance of conventional (two-symbol observation) optimum DQPSK is also 2.323 dB worse than coherent detection of differentially encoded BPSK (or QPSK), we conclude that the limiting asymptotic behavior of DOQPSK as considered in this article is at most 3 dB worse than the latter.

V. Comparison with Previous Methods

In [11], a delay-and-multiply form of receiver for differential detection of OQPSK was proposed. Specifically, using the identical differentially encoded OQPSK modulation as in Fig. 2 or, equivalently, Fig. 3, the receiver, which is illustrated here in Fig. 6, was shown to be appropriate for making bit-by-bit decisions on the information bits $\{c_n\}$. While receivers of this type have the implementation advantage of not requiring quadrature carrier demodulation references, they do require a specific relationship between the radian carrier frequency ω_c and bit time T_b, specifically, in this instance, $\omega_c T_b = 2k\pi$. Also note that, by a simple modification of the value of $\omega_c T_b$, i.e., now choose $\omega_c T_b = 2k\pi + \pi/4$, the receiver of Fig. 6 can be simplified as in Fig. 7. To establish the equivalence between the receivers in Figs. 6 and 7, we note that if the noise-free received signal is expressed as $r(t) = \sqrt{E_b/T_b}\cos(\omega_c t + \phi(t))$, then since $\omega_c T_b = 2k\pi$, the inputs to the I and Q lowpass filters (ignoring second harmonics of the carrier) in Fig. 6 are

$$\left.\begin{aligned} \varepsilon_I(t) &= \frac{1}{2}\sqrt{\frac{E_b}{T_b}}\cos\left(\omega_c T_b + \Delta\phi(t)\right) = \frac{1}{2}\sqrt{\frac{E_b}{T_b}}\cos\left(\Delta\phi(t)\right) \\ \varepsilon_Q(t) &= \frac{1}{2}\sqrt{\frac{E_b}{T_b}}\sin\left(\omega_c T_b + \Delta\phi(t)\right) = \frac{1}{2}\sqrt{\frac{E_b}{T_b}}\sin\left(\Delta\phi(t)\right) \end{aligned}\right\} \tag{39}$$

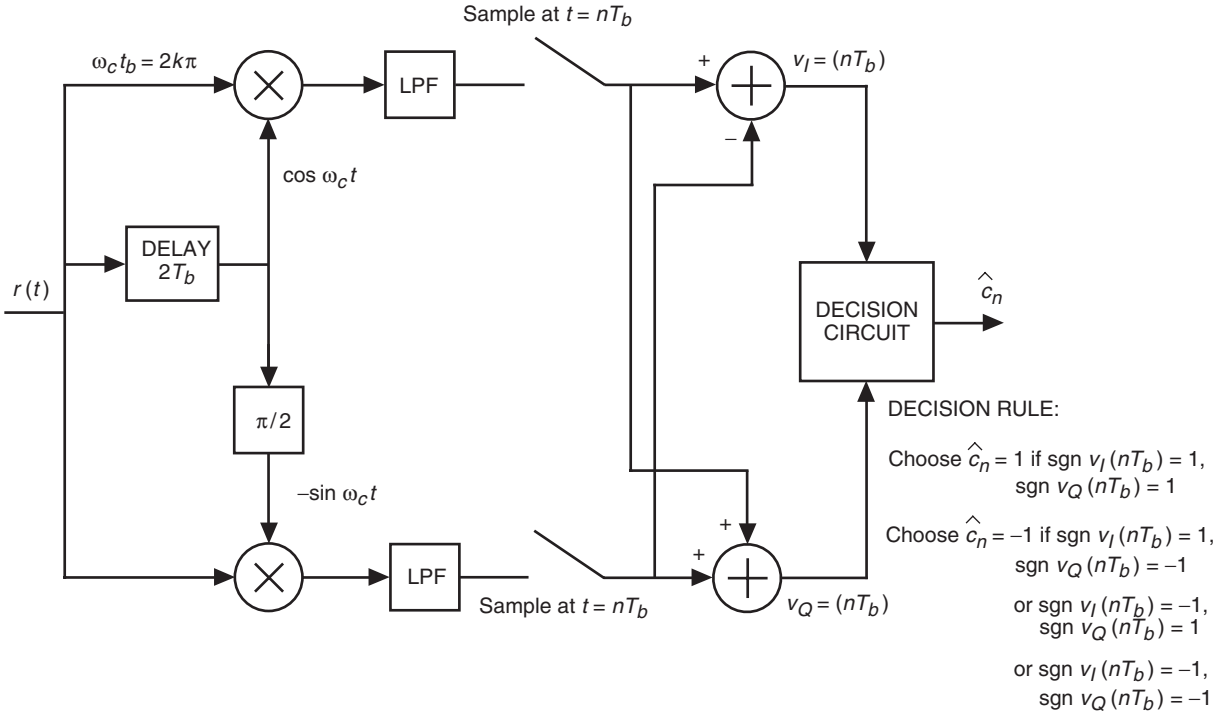

Fig. 6. Delay-and-multiply form of receiver for DOQPSK.

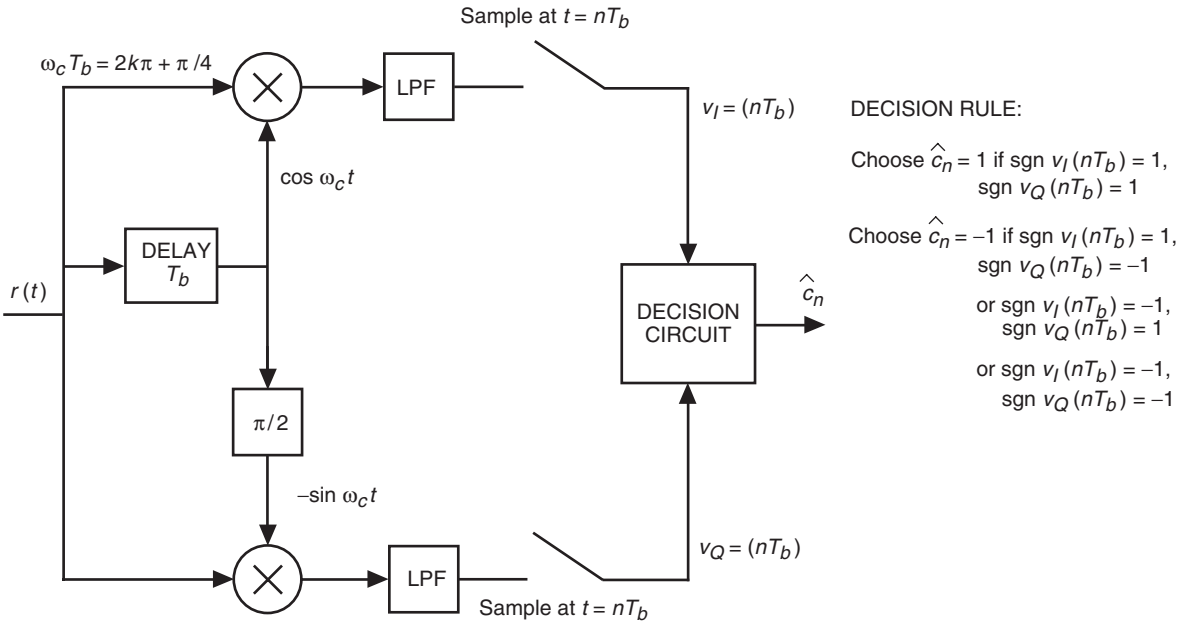

Fig. 7. Simplified version of delay-and-multiply form of receiver for DOQPSK.

where $\Delta\phi(t) = \phi(t) - \phi(t - T_b)$ is the differentially encoded phase and takes on values $(0, \pi/2, \pi, 3\pi/2)$. Moreover, the I and Q decision variables (samples) for the nth bit interval are

$$\left.\begin{aligned} v_I(nT_b) &= \varepsilon_I(nT_b) - \varepsilon_Q(nT_b) = \frac{1}{2}\sqrt{\frac{E_b}{T_b}}\left[\cos(\Delta\phi_n) - \sin(\Delta\phi_n)\right] \\ &= \frac{1}{2\sqrt{2}}\sqrt{\frac{E_b}{T_b}}\cos\left(\Delta\phi_n + \frac{\pi}{4}\right) \\ v_Q(nT_b) &= \varepsilon_I(nT_b) + \varepsilon_Q(nT_b) = \frac{1}{2}\sqrt{\frac{E_b}{T_b}}\left[\cos(\Delta\phi_n) + \sin(\Delta\phi_n)\right] \\ &= \frac{1}{2\sqrt{2}}\sqrt{\frac{E_b}{T_b}}\sin\left(\Delta\phi_n + \frac{\pi}{4}\right) \end{aligned}\right\} \tag{40}$$

where $\Delta\phi_n = \Delta\phi(nT_b)$. Taking into account the fact that now $\omega_c T_b = 2k\pi + \pi/4$, the equivalent inputs to the I and Q lowpass filters in Fig. 7 are

$$\left.\begin{aligned} \varepsilon_I(t) &= \frac{1}{2}\sqrt{\frac{E_b}{T_b}}\cos\left(\omega_c T_b + \Delta\phi(t)\right) = \frac{1}{2}\sqrt{\frac{E_b}{T_b}}\cos\left(\Delta\phi(t) + \frac{\pi}{4}\right) \\ \varepsilon_Q(t) &= \frac{1}{2}\sqrt{\frac{E_b}{T_b}}\sin\left(\omega_c T_b + \Delta\phi(t)\right) = \frac{1}{2}\sqrt{\frac{E_b}{T_b}}\sin\left(\Delta\phi(t) + \frac{\pi}{4}\right) \end{aligned}\right\} \tag{41}$$

which when sampled at $t = nT_b$ produce (except for a scale factor) the same decision variables as in Eq. (40). Finally, as noted in [11], although in the absence of noise the pair of decision variables

$[\text{sgn}\, v_I(nT_b), \text{sgn}\, v_Q(nT_b)]$ can assume only three possible states, namely, $(1,1), (1,-1), (-1,1)$, the first being assigned to $c_n = 1$ and the second two to $c_n = -1$,[11] in the presence of noise the state $(-1,-1)$ is also possible and thus must be assigned to the decision $c_n = -1$.

Although the receiver of Fig. 6 (or its equivalent in Fig. 7) was proposed and demonstrated to be appropriate for decision making in [11], its performance was never given or even discussed. Rather than derive the performance of this receiver per se, we propose a matched-filter version of it, as illustrated in Fig. 8, whose complex baseband form resembles the type of receiver that we have considered in this article and whose average BEP performance can be determined from an analysis similar to that used for evaluating the performance of the optimum receiver of DQPSK. In particular, we first note that, in view of the form of the quadrature decision variables in Eq. (40), the decision rule in Figs. 6 and 7 can be restated in terms of angular decision regions as follows:

$$\left.\begin{array}{l} \text{Choose } \hat{c}_n = 1 \text{ if } 0 \le \tan^{-1}\dfrac{v_Q(nT_b)}{v_I(nT_b)} \le \dfrac{\pi}{2} \\ \\ \text{Otherwise, choose } \hat{c}_n = -1 \end{array}\right\} \tag{42}$$

Since $\tan^{-1}[v_Q(nT_b)/v_I(nT_b)]$ is a noisy measure of $\Delta\phi(nT_b)+\pi/4$ and since in Fig. 8 the phase estimate difference $\Delta\eta_n \triangleq \eta_n - \eta_{n-1} = \tan^{-1}(V_{Qn}/V_{In}) - \tan^{-1}(V_{Q,n-1}/V_{I,n-1})$ is a noisy measure of $\Delta\phi(nT_b)$ (i.e., without the $\pi/4$ rotation), then by analogy with Eq. (42) the equivalent decision rule for this receiver is

$$\left.\begin{array}{l} \text{Choose } \hat{c}_n = 1 \text{ if } -\dfrac{\pi}{4} \le \Delta\eta_n \le \dfrac{\pi}{4} \\ \\ \text{Otherwise, choose } \hat{c}_n = -1 \end{array}\right\} \tag{43}$$

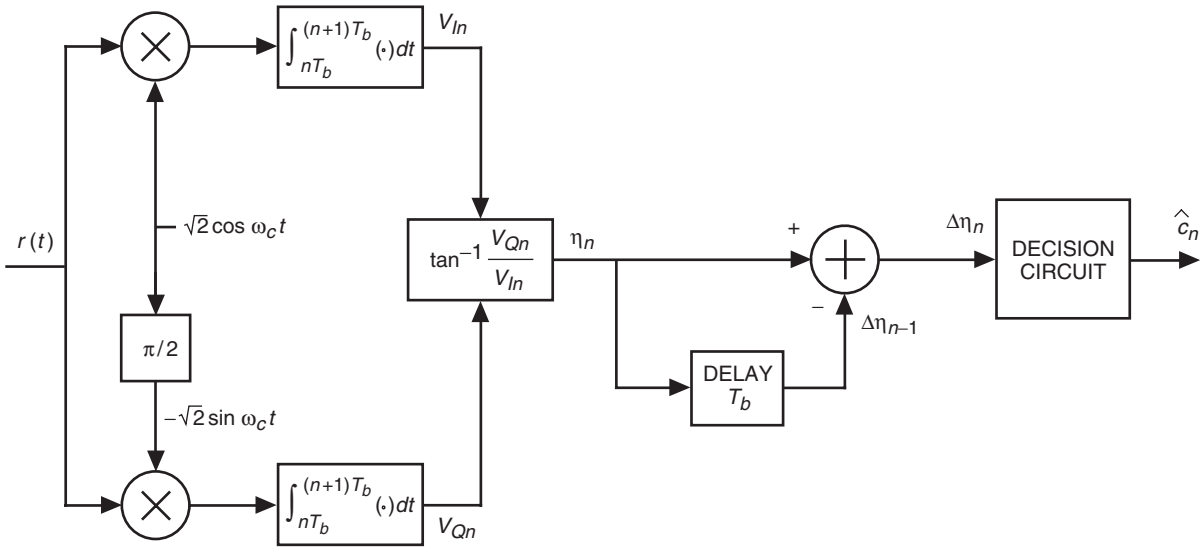

Fig. 8. A matched-filter version of the receiver in Fig. 6.

[11] In this sense, the decision rule resembles that in Eq. (15) in that it transforms a pair of decision variables having three possible states into a binary decision.

Based on the above decision rule, the average BEP of the receiver in Fig. 8 is given by

$$P_b(E) = \frac{1}{2}P_{b1}(E) + \frac{1}{2}P_{b,-1}(E) \tag{44}$$

where

$$\left.\begin{aligned} P_{b1}(E) &= 1 - \Pr\left\{-\frac{\pi}{4} \le \Delta\eta_n \le \frac{\pi}{4}\,\middle|_{\substack{c_n=1\\(\Delta\phi_n=0)}}\right\} = 1 - \Pr\left\{-\frac{\pi}{4} \le \Delta\eta_n - |\Delta\phi| \le \frac{\pi}{4}\right\} \\ P_{b,-1}(E) &= \Pr\left\{-\frac{\pi}{4} \le \Delta\eta_n \le \frac{\pi}{4}\,\middle|_{\substack{c_n=-1\\(\Delta\phi_n=\pm\frac{\pi}{2})}}\right\} = \Pr\left\{-\frac{3\pi}{4} \le \Delta\eta_n - |\Delta\phi| \le -\frac{\pi}{4}\right\} \\ &= 1 - \Pr\left\{-\frac{\pi}{4} \le \Delta\eta_n - |\Delta\phi| \le \frac{\pi}{4}\right\} - \Pr\left\{\frac{\pi}{4} \le \Delta\eta_n - |\Delta\phi| \le \frac{5\pi}{4}\right\} \end{aligned}\right\} \tag{45}$$

Letting $\psi = \Delta\eta_n - |\Delta\phi|$, then substituting Eq. (45) in Eq. (44) gives

$$P_b(E) = 1 - \Pr\left\{-\frac{\pi}{4} \le \psi \le \frac{\pi}{4}\right\} - \frac{1}{2}\Pr\left\{\frac{\pi}{4} \le \psi \le \frac{5\pi}{4}\right\} \tag{46}$$

Comparing Fig. 8 for DOQPSK with the optimum DQPSK receiver [16, Fig. 7.1], we conclude that the statistics of ψ are identical for the two except for a 3-dB difference in SNR due to the fact that the I&Ds in the former operate over a bit time whereas the I&Ds in the latter operate over a symbol time. Thus, following an analysis approach similar to that taken in [16, Chap. 7], we find that the average BEP as determined from Eq. (46) is given by

$$P_b(E) = \frac{3}{2}\frac{1}{4\sqrt{2}\pi}\int_{-\pi/2}^{\pi/2}\frac{\exp\left\{-\frac{E_b}{N_0}\left[1-\frac{1}{\sqrt{2}}\cos t\right]\right\}}{1-\frac{1}{\sqrt{2}}\cos t}dt - \frac{1}{2}\frac{1}{4\sqrt{2}\pi}\int_{-\pi/2}^{\pi/2}\frac{\exp\left\{-\frac{E_b}{N_0}\left[1+\frac{1}{\sqrt{2}}\cos t\right]\right\}}{1+\frac{1}{\sqrt{2}}\cos t}dt \tag{47}$$

By comparison, for DQPSK with a Gray code mapping of bits to symbols, the average BEP is exactly obtained from [16, Eq. (7.16a)] as

$$P_b(E) = \frac{1}{4\sqrt{2}\pi}\int_{-\pi/2}^{\pi/2}\frac{\exp\left\{-\frac{2E_b}{N_0}\left[1-\frac{1}{\sqrt{2}}\cos t\right]\right\}}{1-\frac{1}{\sqrt{2}}\cos t}dt - \frac{1}{4\sqrt{2}\pi}\int_{-\pi/2}^{\pi/2}\frac{\exp\left\{-\frac{2E_b}{N_0}\left[1+\frac{1}{\sqrt{2}}\cos t\right]\right\}}{1+\frac{1}{\sqrt{2}}\cos t}dt \tag{48}$$

Since at a high SNR the first of the two terms in Eqs. (47) and (48) dominates, then ignoring the factor of 3/2 in Eq. (47), we conclude that the DOQPSK receiver of Fig. 8 is 3 dB worse in performance than the optimum receiver of DQPSK. This conclusion is the same as that previously stated for the multiple-bit differential detection receiver corresponding to $N = 2$.

VI. Extension to Shaped OQPSK (SOQPSK)

In [21], shaped BPSK (SBPSK) was introduced as a means of bandlimiting a BPSK signal while, at the same time, keeping its envelope constant. Further development of the SBPSK concept led to a variant of this scheme for offset quadrature modulation, referred to as shaped offset QPSK (SOQPSK). Simply put, SOQPSK is an OQPSK modulation in which the phase transitions occur smoothly rather than abruptly and as such provides improved spectral efficiency over OQPSK when used on a nonlinear channel. From a mathematical standpoint, SOQPSK can be represented by the precoded CPM modulator of Fig. 1, where the phase pulse shape $q(t)$ is no longer restricted to be a step function.[12]

In the original conception of SOQPSK, a rectangular frequency pulse of duration equal to the bit period was used for $g(t)$, i.e., $g(t) = 1/(2T_b),\ 0 \le t \le T_b$, corresponding to the phase pulse $q(t) = t/2T_b,\ 0 \le t \le T_b$ and $q(t) = 1/2,\ T_b \le t \le \infty$. In this sense, one might think that SOQPSK resembles minimum-shift keying (MSK) [16, Chap. 10]; however, we remind the reader that, for the latter, the data alphabet $\{\alpha_i\}$ is fixed at $-1,+1$, whereas for the former it varies between $0,-1$ and $0,+1$. Thus, whereas in a given bit interval the phase for MSK is always linearly varying with either a positive or negative slope, the phase for SOQPSK can either vary linearly or remain stationary. This behavior is easily seen in the SOQPSK trellis diagram provided in Fig. 9.

Based upon the above discussion, it is easily shown that the MLSE decision rule for SOQPSK with unit bit-duration frequency pulse is still given as in Eq. (10) together with Eq. (11), where now

$$\Gamma_n = \int_{nT_b}^{(n+1)T_b} \tilde{R}(t) \exp\left\{-j\pi\alpha_n \left[q(t-nT_b) - \frac{1}{2}\right]\right\} dt \tag{49}$$

and C_n is still defined as in Eq. (13). In particular, for the rectangular frequency pulse as above, Eq. (49) becomes

$$\Gamma_n = \int_{nT_b}^{(n+1)T_b} \tilde{R}(t) \exp\left\{-j\pi\alpha_n \left[\frac{t-(n+1)T_b}{2T_b}\right]\right\} dt \tag{50}$$

It should be noted that, because the Γ_n's now depend on the α_n's, the metric of Eq. (11) now depends on α_{n-N+1} in addition to $\alpha_{n-N+2}, \cdots, \alpha_{n-1}, \alpha_n$ as before for OQPSK and, thus, *an observation of N bits now results in a decision on N bits,* as was the case for pure CPM in [15]. Alternatively, the N-bit observation intervals no longer need overlap.

To evaluate the PEP for SOQPSK, it should be clear that the generic form still is given by Eq. (20), where in view of the modification of Eq. (12) to Eq. (49), the parameter δ of Eq. (22) is now given by

$$\delta = \sum_{l=0}^{N-1} j^{\sum_{m=0}^{N-l-2} \Delta\alpha_{n-l-m}} \left(\frac{1}{T_b}\int_{nT_b}^{(n+1)T_b} \exp\left\{j\pi\Delta\alpha_{n-l}\left[q(t-nT_b) - \frac{1}{2}\right]\right\} dt\right) \tag{51}$$

With no loss of generality, we may set $n = 0$ in Eqs. (51) and (52) as was done in [15]. For the square frequency pulse, the integral can be evaluated in closed form in terms of trigonometric functions, resulting in [15]

[12] The frequency pulse $g(t)$ still must be normalized so that the corresponding phase pulse satisfies $q(t) = \int_0^{LT_b} g(\tau)\, d\tau = 1/2$, where LT_b is the duration of $g(t)$. A choice of $g(t)$ corresponding to a single bit time ($L = 1$) results in a full-response CPM representation.

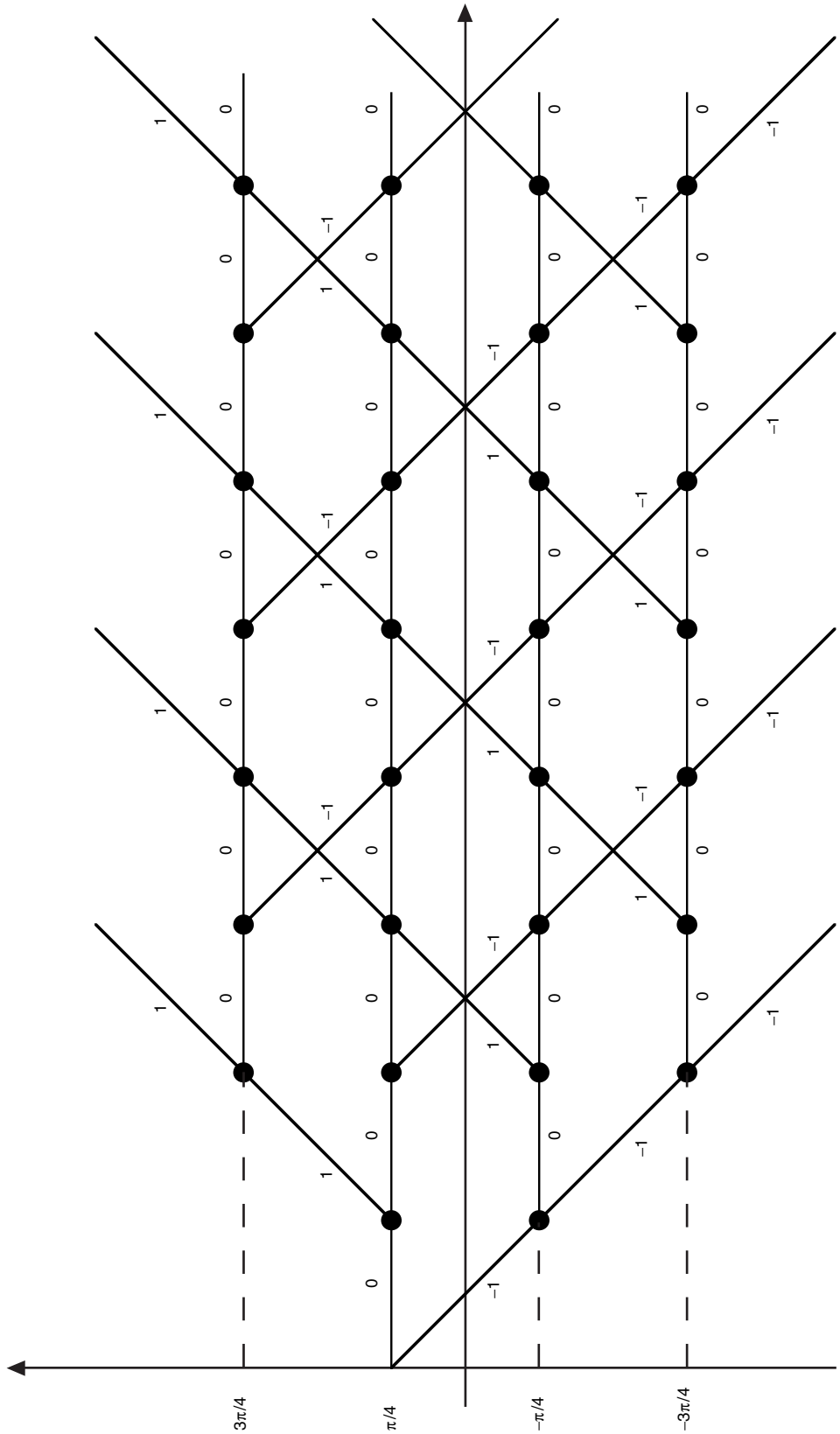

Fig. 9. Phase trellis diagram for SOQPSK (branches are labeled with values of α_i).

$$\delta = \sum_{l=0}^{N-1} j^{\sum_{m=0}^{N-l-2} \Delta\alpha_{-l-m}} \left(\frac{1}{T_b} \int_0^{T_b} \exp\left[j\pi\Delta\alpha_{-l} \left(\frac{t-T_b}{2T_b} \right) \right] dt \right)$$

$$= \sum_{l=0}^{N-1} j^{\sum_{m=0}^{N-l-2} \Delta\alpha_{-l-m}} \left(\frac{\sin\frac{\pi\Delta\alpha_{-l}}{4}}{\frac{\pi\Delta\alpha_{-l}}{4}} \right) \exp\left(-j\frac{\pi\Delta\alpha_{-l}}{4} \right) \tag{52}$$

As an example, for $N = 2$ there are now are a total of 36 possible error sequence pairs resulting in 4 different values of $|\delta|^2$, namely, $|\delta_1|^2 = 1 + 4/\pi + 8/\pi^2$, $|\delta_2|^2 = 4/\pi^2$, $|\delta_3|^2 = 16/\pi^2$, and $|\delta_4|^2 = 32/\pi^2$, with corresponding PEPs computed from Eq. (20) as

$$\mathrm{PEP}_i = \frac{1}{2} \left[1 - Q\left(\sqrt{\frac{E_b}{N_0}\left(1 + \sqrt{1 - \frac{1}{4}|\delta_i|^2} \right)}, \sqrt{\frac{E_b}{N_0}\left(1 - \sqrt{1 - \frac{1}{4}|\delta_i|^2} \right)} \right) \right.$$

$$\left. + Q\left(\sqrt{\frac{E_b}{N_0}\left(1 - \sqrt{1 - \frac{1}{4}|\delta_i|^2} \right)}, \sqrt{\frac{E_b}{N_0}\left(1 + \sqrt{1 - \frac{1}{4}|\delta_i|^2} \right)} \right) \right], \; i = 1,2,3,4,5 \tag{53}$$

The accumulated values of $w(\mathbf{c},\hat{\mathbf{c}})\,P(\mathbf{c},\hat{\mathbf{c}})$ for these PEPs are $w(\mathbf{c},\hat{\mathbf{c}})\,P(\mathbf{c},\hat{\mathbf{c}})_1 = 6$, $w(\mathbf{c},\hat{\mathbf{c}})\,P(\mathbf{c},\hat{\mathbf{c}})_2 = 2$, $w(\mathbf{c},\hat{\mathbf{c}})\,P(\mathbf{c},\hat{\mathbf{c}})_3 = 6$, and $w(\mathbf{c},\hat{\mathbf{c}})\,P(\mathbf{c},\hat{\mathbf{c}})_4 = 2$. Finally then, the upper bound on average BEP is given by

$$P_b(E) \le 6\mathrm{PEP}_1 + 2\mathrm{PEP}_2 + 6\mathrm{PEP}_3 + 2\mathrm{PEP}_4 \tag{54}$$

If one is again interested in asymptotic behavior, then, as before, the dominant terms in the average BEP occur for the sequences that result in the minimum value of $N - |\delta|$, or, equivalently, the maximum value of $|\delta|$. Here the maximum value of $|\delta|$ occurs for the error sequence $\hat{\boldsymbol{\alpha}}$ having $\Delta\alpha_{-N+1} = \Delta\alpha_{-N+2} = \cdots = \Delta\alpha_{-1} = 0$ and $\Delta\alpha_0 = \pm 1$, which from Eq. (52) evaluates to[13]

$$|\delta|_{\max} = \sqrt{\left(N - 1 + \frac{2}{\pi} \right)^2 + \left(\frac{2}{\pi} \right)^2} = \sqrt{(N-1)^2 + \frac{4}{\pi}(N-1) + \frac{8}{\pi^2}} \tag{55}$$

Hence, from Eqs. (19) and (30), the average BEP would be approximately upper bounded by

$$P_b(E) \lesssim \left(\sum_{\mathbf{c}\neq\hat{\mathbf{c}}} \sum w(\mathbf{c},\hat{\mathbf{c}})\,P(\mathbf{c},\hat{\mathbf{c}}) \right) \frac{1}{N-1} \frac{1}{2^{N-1}} \sqrt{\frac{N + |\delta|_{\max}}{8\,|\delta|_{\max}}}\, \mathrm{erfc}\left(\sqrt{\frac{E_b}{2N_0}\left(N - |\delta|_{\max} \right)} \right) \tag{56}$$

with $|\delta|_{\max}$ as above. Here again the $w(\mathbf{c},\hat{\mathbf{c}})\,P(\mathbf{c},\hat{\mathbf{c}})$ terms in the double summation correspond only to those error sequence pairs, of which there are $4N_s$ [N_s as defined in Eq. (16)], that result in $|\delta|_{\max}$. If

[13] For the case $N = 2$, the maximum value of $|\delta|$ actually occurs for the sequence $\Delta\alpha_{-1} = 1, \Delta\alpha_0 = -1$ or $\Delta\alpha_{-1} = -1, \Delta\alpha_0 = 1$ and is given by $|\delta|_{\max} = 4\sqrt{2}/\pi$ in accordance with what was previously denoted below Eq. (52) as $|\delta_4|$.

we again define the asymptotic coding gain (in dB) in terms of the argument of the complementary error relative to its value for $N = 2$, then based on the above we have

$$G = 10 \log_{10} \frac{N - \sqrt{(N-1)^2 + \frac{4}{\pi}(N-1) + \frac{8}{\pi^2}}}{2 - \frac{4\sqrt{2}}{\pi}}, \quad N \geq 3 \tag{57}$$

Finally, since

$$\lim_{N \to \infty} N - \sqrt{(N-1)^2 + \frac{4}{\pi}(N-1) + \frac{8}{\pi^2}} = 1 \tag{58}$$

then in the limit of large observation time, the asymptotic behavior of multiple-bit differential detection of SOQPSK behaves identically to that of DOQPSK. For any finite N, however, the performance of differentially detected SOQPSK would be worse than that of DOQPSK since the quantity $N - |\delta|_{\max}$ is smaller [see Eq. (55)] for the former than it is for the latter [see Eq. (35)].

VII. Conclusions

Based on a CPM representation for differentially encoded offset QPSK, we have derived and given the average BEP performance of a receiver that performs differential detection of this modulation. Since the receiver is derived from maximum-likelihood considerations, it is expected to be the most power efficient of its type. Based on its resemblance to multiple-symbol detection of nonoffset QPSK, the performance of the receiver continues to improve as a function of the observation length (as measured in bit intervals) of the received signal. When compared with the optimum DQPSK receiver, which bases its decision on the difference of two symbols, thus requiring observation of the received signal over two symbol (or, equivalently, four bit) intervals, the proposed DOQPSK receiver with a 4-bit observation has an asymptotic SNR penalty of 1.446 dB. In the limit of large SNR, whereas multiple-symbol differential detection of QPSK approaches the performance of coherently detected BPSK with differential encoding, multiple-bit differential detection of OQPSK has a similar limiting behavior but with a penalty of 3 dB. The same limiting behavior has also been demonstrated for spectrally shaped OQPSK with linear phase variation. Extension of the method to differential detection of more bandwidth-efficient forms of SOQPSK [22] with precoded *partial* response CPM representations [17] is possible but somewhat more complex because of the increase in the number of trellis states.

Acknowledgments

The author is indebted to Mr. Dennis Lee of the Jet Propulsion Laboratory and Dr. Dariush Divsalar of Sequoia Communications and the Jet Propulsion Laboratory for many stimulating and informative technical discussions relative to the subject of interest.

References

[1] M. K. Simon and D. Divsalar, "Multiple Symbol Differential Detection of MPSK," *IEEE Trans. Commun.,* vol. 38, no. 3, pp. 300–308, March 1990. Also to appear in the IEEE Communications Society 50th Anniversary Journal Collection.

[2] S. G. Wilson, J. Freebersyser, and C. Marshall, "Multi-Symbol Detection of M-DPSK," *GLOBECOM '89 Conf. Rec.,* Dallas, Texas, pp. 47.3.1–47.3.6, November 27–30, 1989.

[3] K. Mackenthun, "A Fast Algorithm for Multiple-Symbol Differential Detection of MPSK," *IEEE Trans. Commun.,* vol. 42, no. 2, pp. 1471–1474, February/March/April 1994.

[4] F. Edbauer, "Bit Error Rate of Binary and Quaternary DPSK Signals with Multiple Decision Feedback Detection," *IEEE Trans. Commun.,* vol. 40, no. 3, pp. 457–460, March 1992.

[5] P. Tarasak and V. K. Bhargava, "Reduced Complexity Multiple Symbol Differential Detection of Space–Time Block Code," *Wireless Commun. and Network. Conf.,* WCNC2002, vol. 1, Orlando, Florida, pp. 505–509, March 17–21, 2002.

[6] D. Lao and A. M. Haimovich, "Performance Comparison of Multiple-Symbol Differential Detection and Optimum Combining, *IEEE Internat. Conf. On Commun.,* ICC2002, New York, pp. 257–261, April 28–May 2, 2002.

[7] D. T. Lee, O. S. Uhm, and H. S. Lee, "Differentially Coherent Communication with Multiple-Symbol Observation Interval," *IEEE Commun. Lett.,* vol. 5, no. 1, pp. 1–3, January 2001.

[8] P. Fan, "Multiple-Symbol Detection for Transmit Diversity with Differential Encoding Scheme," *IEEE Trans. Consumer Electr.,* vol. 47, no. 1, pp. 96–100, February 2001.

[9] M. K. Simon and M.-S. Alouini, "Multiple Symbol Differential Detection with Diversity Reception," *IEEE Trans. Commun.,* vol. 49, no. 8, pp. 1312–1319, August 2001.

[10] L. H.-J. Lampe and R. F. H. Fischer, "Low Complexity Multilevel Coding for Multiple-Symbol Differential Detection," *Electr. Lett.,* vol. 36, no. 25, pp. 2081–2082, December 7, 2000.

[11] K. Defly, M. Lecours, and N. Boutin, "Differential Detection of the OQPSK Signal: Coding and Decoding," *IEEE Internat. Conf. On Commun.,* ICC1989, Boston, Massachusetts, pp. 54.3.1–54.3.1, June 11–14, 1989.

[12] S. Hischke, J. Habermann, and R. Comley, "Receivers for Differentially Encoded OQPSK—A Comparison of Differential Demodulation with Joint Data and Channel Estimation," *Proc. IEEE Int. Conf. on Telecommunications,* Melbourne, Australia, pp. 1055–1060, 1997.

[13] P. A. Baker, "Phase Modulation Data Sets for 2000 and 2400 Bits per Second, Part 1," *AIAA Trans. Commun. Electr.,* pp. 166–171, July 1962.

[14] F. Xiong and D. Wu, "Multiple-Symbol Differential Detection of $\pi/4$-DQPSK in Land Mobile Satellite Communication Channels," *IEE Proc.,* vol. 147, no. 3, pp. 163–168, June 2000.

[15] M. K. Simon and D. Divsalar, "Maximum-Likelihood Block Detection of Noncoherent Continuous Phase Modulation," *IEEE Trans. Commun.,* vol. 41, no. 1, pp. 90–98, January 1993.

[16] M. K. Simon, S. Hinedi, and W. C. Lindsey, *Digital Communication Techniques: Signal Design and Detection,* Upper Saddle River, New Jersey: Prentice Hall, 1995.

[17] M. K. Simon, *Bandwidth-Efficient Digital Modulation with Application to Deep-Space Communications,* Monograph 3, JPL Deep Space Communications and Navigation (DESCANSO) Monograph Series, Jet Propulsion Laboratory, Pasadena, California, June 2001.
http://descanso.jpl.nasa.gov/

[18] S. Stein, "Unified Analysis of Certain Coherent and Noncoherent Binary Communication Systems," *IEEE Trans. Inform. Theory,* vol. 1, pp. 43–51, January 1964.

[19] J. B. Anderson, T. Aulin, and C.-E. Sundberg, *Digital Phase Modulation,* New York: Plenum Press, 1986.

[20] J. I. Marcum, "Table of Q Functions," U.S. Air Force Project RAND Research Memorandum M-339, ASTIA Document AD 1165451, Rand Corporation, Santa Monica, California, January 1, 1950.

[21] M. J. Dapper and T. J. Hill, "SBPSK: A Robust Bandwidth-Efficient Modulation for Hard-Limited Channels," *MILCOM Conf. Rec.,* Los Angeles, California, pp. 31.6.1–31.6.6, October 21–24, 1984.

[22] T. J. Hill, "An Enhanced, Constant Envelope, Interoperable Shaped Offset QPSK (SOQPSK) Waveform for Improved Spectral Efficiency," International Telemetering Conf., San Diego, California, October 23–26, 2000. Also see T. J. Hill, "A Non-Proprietary, Constant Envelope, Variant of Shaped Offset QPSK (SOQPSK) for Improved Spectral Containment and Detection Efficiency," *MILCOM Conf. Rec.,* Los Angeles, California, pp. 347–352, October 23–26, 2000.